TECHNICAL MEMORANDUM

256

The forecast impact of changes to the albedo of the boreal forests in the presence of snow

P. Viterbo and A. Betts

Research Department

August 1998

European Centre for Medium-Range Weather Forecasts
Europäisches Zentrum für mittelfristige Wettervorhersage
Centre européen pour les prévisions météorologiques à moyen

THE FORECAST IMPACT OF CHANGES TO THE ALBEDO OF THE BOREAL FORESTS IN THE PRESENCE OF SNOW

Pedro Viterbo and Alan K. Betts

Abstract

A change in the calculation of the albedo for the boreal forests in the presence of snow in the ECMWF model, which reduces the deep snow albedo from 0.8 to 0.2, greatly reduces the model systematic cold temperature bias both at the surface and in the lower troposphere at high northern latitudes in the Spring.

1. INTRODUCTION

For several years, the spring time 2-m temperature forecasts from the European Centre for Medium-Range Weather Forecasts (ECMWF) for high northern latitudes have had a systematic cold bias in the presence of snow. It has been suggested by several research groups that the model cannot effectively distinguish snow over bare ground and the snow hidden below the forest canopy. During the April 1996 Intensive Observation Period of BOREAS (Boreal Ecosystem-Atmosphere Study) in the Canadian boreal forest, the ECMWF day time forecast of near-surface temperatures were 10 to 15 K colder than observations [*Sellers et al.*, 1997]. A time series of the model albedo, together with the observed and ECMWF model 36-hour forecast 2-m temperatures for the beginning of April 1996 in the BOREAS southern study area in Saskatchewan, Canada, shown in Figure 1, points directly to the source of the problem. The heavy dashed curve is the model forecast temperature at 53.63°N, 106.2°W, the location of the Old Aspen site in the Prince Albert National Park (shown as a light solid curve) and the heavy solid line is at the Old Jack Pine site nearby to the north-east at 53.92°N, 104.69°W. At the beginning of April, when there is snow in the model (and on the ground), the model albedo is close to 0.8 and there is a strong cold bias of about 10K on most days at 0000 UTC, which is at the end of the diurnal heating cycle (1800 local time) for the preceding Julian day. Generally the coniferous site, which has a lower albedo [*Betts and Ball,* 1997], is warmer than the deciduous aspen site. The times for which the cold bias is less (0000 UTC on April 3, 7, 10) follow cloudy days when the observed diurnal rise of temperature is small. When the snow "melts" (which happens in the model on 960412), the forecast albedo decreases to its background value of 0.12, and the forecast temperature becomes much closer to observations.

Some ground truth estimates for the albedo at selected sites are given in *Betts and Ball* [1997], who studied the annual cycle of albedo for 1994 and 1995 at ten BOREAS mesonet sites located over grass, the aspen forest and the coniferous forests, using data from upward and downward looking pyranometers mounted on towers above the canopy. Representative winter values for daily averaged albedo of snow-covered grass sites are 0.75, while corresponding values for the aspen and conifer sites are 0.21 and 0.13 respectively, with a few values as high as 0.4, 24 to 48 hours after snowfall. In the winters studied, the albedo of the aspen (coniferous) sites exceeded 0.3 (0.2) for about ten 2-day periods, following high snowfall situations, decreasing quickly to the representative winter values after the intercepted snow melts or blows off with the wind. Data from other observational studies in forest areas corroborate these results [*Robinson and Kukla*, 1984; *Harding and Pomeroy,*1996; *Pomeroy and Dion*, 1996]. The surprisingly few attempts of making a hemispheric satellite based estimate of albedo (e.g., *Laine and Heikinheimo* [1996], and *Robinson and Kukla*

[1985]), suggest lower albedos over the boreal forests than in adjacent forest free areas, although the absolute values of these estimates might be questionable due to cloud-clearing problems (essentially it is very hard to distinguish a low cloud from the snow-covered surface below).

The above evidence suggested that a new treatment of the boreal forest albedo in the presence of snow (hereafter the "snow albedo"), effectively distinguishing forest covered and forest free areas, was necessary in the model. This paper describes the changes made to the snow albedo scheme and the extensive experimentation done. In section 2, we outline the old and new snow albedo treatments: some more details are given in an Appendix. Section 3 presents the forecast impact in spring, including 2-m temperatures, scores and systematic errors, and section 4 presents the impact on an ensemble of long runs in Spring. This new snow albedo scheme was implemented in the operational model on December 10, 1996. In conclusion we show the large reduction in the 850 hPa cold temperature bias in the operational ECMWF model over the boreal forest between Spring 1996 and Spring 1997.

2. DESCRIPTION OF MODEL CHANGES

2.1 Albedo in operational model before December 1996.

The model forecast albedo in a grid box was a combination of the background albedo over a snow-free grid box fraction, with a calculated snow albedo for the remaining snow-covered fraction. In the operational model, prior to December 1996, this snow albedo was done following a fairly complex series of computations, involving background albedo, snow depth, roughness length, vegetation fraction, surface temperature, and interception reservoir contents. However, the end result of these computations was unsatisfactory as it gave an albedo in the presence of snow that is rarely outside the 0.7- 0.8 range (see Appendix and Figure 3b below).

2.2 Revised snow albedo scheme

The new procedure for defining the snow albedo distinguishes the forests based on their snow-free background albedo (which is a fixed model field, taken from the climatology of *Dorman and Sellers* [1989]). The land points shown shaded in Figure 2a are the areas of the globe covered by forest, where the background albedo, α_B , is less than 15%. Figure 2b, from the ISLSCP (International Satellite Land Surface Climatology Project) data set of *Sellers et al.* [1996] also identifies the forest types with dark shading. The correspondence between the two figures is sufficiently close that we used background albedo to identify forests, rather than introduce another constant field for vegetation type in the model. An albedo for the snow-covered part of the grid box, α_s , is defined as

$$\alpha_s = \min(a_2, \max(a_1, a_1 + c_1(\alpha_B - b_1))) \qquad (1)$$

$$a_1 = 0.2, \quad a_2 = 0.7, \quad b_1 = 0.13, \quad b_2 = 0.15, \quad c_1 = (a_1 - a_2)/(b_1 - b_2)$$

Equation (1) ensures a deep snow albedo of 0.2 for forest covered areas (background albedo smaller than 0.13), of 0.7 for forest free areas (background albedo larger than 0.15), and a linear relationship linking the two. The Appendix gives more details. Note the reduction, from 0.8 to 0.7, between the previous and the new maximum albedo value over snow. The previous value (0.8) is representative of fresh clean snow conditions; the new slightly lower value (0.7) was introduced, because the parametrization does not take into account snow ageing effects.

Figure 3 compares the old (labelled control) and the new model albedo in the first day (960331) of two forecasts with triangular truncation T106. The new albedo values are greatly reduced over the areas identified as forests in Figure 2a. Typical new values in this areas are 0.2, compared with old values in excess of 0.7.

To summarise, the old model albedo over snow covered areas was ineffective in its way of distinguishing forest from non-forest areas; since beyond a relatively small snow depth, the albedo is of the order of 0.7-0.8. The new simple treatment for snow albedo, described above, distinguishes the albedo over forests from the albedo over lower vegetation. The forested areas, defined as areas of small background albedo, have a final model deep snow albedo of 0.2, while over the non-forested areas the corresponding limit is 0.7.

2.3 Operational model cycles

There are three model versions relevant to this paper. The operational model in winter and spring of 1996 was cycle 14R3, and our ensembles of forecasts are initialised with these operational analyses. As well as the forest albedo error, 14R3 had a substantial cold winter temperature bias. This was corrected in cycle 15R5 [*Viterbo et al.* 1998], which introduced soil freezing and changes to the stable boundary layer, as well as increased the coupling between soil and atmosphere. Cycle 15R5 became operational in September 1996, and it is used as the control forecast model for our ensembles, as it contains the old albedo scheme. The model cycle 15R6 contains in addition the modifications to the snow albedo discussed in section 2.2: it became the operational model in December 1996, following the set of experiments described here.

3. FORECAST IMPACT OF ALBEDO CHANGE

The forecast impact is largest in the spring period, when snow lies on the ground and the incoming solar radiation is large. This section describes the results from a set of 40 ten-day forecasts with resolution T106L31 (triangular truncation of T106 and 31 levels in the vertical), which were run with initial conditions from 1200 UTC every third day between 960202 and 960529 for cycle 15R5 (designated CONTROL), and the new albedo scheme, 15R6 (designated NEW). These forecasts are initialised with the available operational analysis (14R3), which has a substantial cold soil and surface temperature bias. In section 3.2 we show the additional beneficial impact of correcting this soil temperature error.

3.1 2-m temperature errors

Figure 4 shows the verification of 2-m temperature for the eleven 60-hour forecasts (corresponding to 0000 UTC) with initial dates between 960315 and 960414, over the northern part of the North American continent. The upper panel is the 15R5 Control forecast, where the numbers show that the mean temperature errors are of order -10K. The centre panel is with the new albedo scheme and the lower panel shows the difference, where points that now fit the data better are shown in green. Over the Canadian boreal forest, the forecast error is reduced from -9 to -12K to around -2 to -3K. Most of the temperature errors in the new albedo panel lie within the interval -2 to 2K, although a few points around Hudson's Bay are now too warm. 72-hour forecasts over Asia and Northern Europe (not shown) show very similar benefits, with a large improvement in Asia, where the warming at the surface exceeds 10 K over a very large area. Statistics from the above 3 areas are summarised in Table 1 below.

The control forecasts in the whole ensemble were 15R5, starting from the (cold) operational soil temperatures, given by the 14R3 analysis. Although 15R5 includes soil water freezing and changes to the stable layer parameterisation, the effect of these changes is small in these short-term forecasts. Consequently, although the new snow albedo reduces the cold bias, it is not completely removed.

		bias	standard deviation
Northern Europe (72h)	15R5 (CONTROL)	-4.16	5.80
	15R6 (NEW)	-2.25	3.95
Asia (72h)	15R5 (CONTROL)	-7.63	6.57
	15R6 (NEW)	-2.66	4.03
North America (60h)	15R5 (CONTROL)	-3.59	5.74
	15R6 (NEW)	-0.69	3.86

Table 1. Statistics on the comparison of 2-m temperature against observations, for all forecasts verifying between 960315 and 960414. Hour 72 forecasts for Asia and Northern Europe, hour 60 for North America. All forecasts are initialised with the 14R3 operational analysis.

3.2 Impact of soil temperature error

To assess separately the impact of the cold soil temperature error in the analysis, we ran 3 forecasts with initial date 960401, with the results summarised in Table 2. Cycle 14R3 is the operational forecast. In the development of 15R5 a long "soil temperature assimilation" run was made [*Viterbo et al.*, 1998] for the full winter of 1996 to obtain corrected soil temperatures. We inserted these soil temperatures into the analysis for 960401 and made the other two forecasts in Table 2, one labelled 15R5 (T_{soil} corrected), and the third one with the snow modifications, 15R6 (T_{soil} corrected).

		bias	standard deviation
Northern Europe 72h	14R3	-4.24	4.51
	15R5 (T_{soil} corrected)	-0.71	4.21
	15R6 (T_{soil} corrected)	0.25	3.61
Asia 72h	14R3	-9.02	7.17
	15R5 (T_{soil} corrected)	-4.38	6.09
	15R6 (T_{soil} corrected)	-0.74	3.37
North America 78h	14R3	-5.54	7.78
	15R5 (T_{soil} corrected)	-2.43	6.57
	15R6 (T_{soil} corrected)	-0.21	4.85

Table 2 Statistics on the Comparison of 2-m Temperature Against Observations for 960401; Hour 72 Forecasts for Asia and Northern Europe, Hour 78 for North America

Results in the table are an illustration of the true separate impact in short term forecasts of the snow albedo changes between cycle 15R5 and 15R6. In both bias and standard deviation, there is a gradual improvement from 14R3 to 15R6, so that with the new snow albedo, the systematic cold bias has been removed.

It is worth noting that the cycle 15R5 modifications to the physics (frozen soil and stable boundary layer) have their maximum impact in winter, when the solar forcing is small, while the albedo modifications described here have their largest impact in the spring season.

3.3 Verification Scores

Figure 5 shows the mean objective scores for the 20 forecasts (Control 15R5 and 15R6 with the new snow albedo) with initial dates in March and April for the northern hemisphere (top) and an east Asian region (bottom). The positive impact on the 850 hPa temperature is global in scale and largest over east Asia. The albedo change reduces the lower tropospheric temperature bias shown on the right hand panels (and with this also reduces the root mean square error), as well as benefiting the anomaly correlation scores shown on the left. Consequently the geopotential height bias (not shown) is reduced. The improved temperature structure over the continents has positive effects downstream (see Figure 7 in section 4), evident from better scores over North Pacific and North Atlantic (not shown).

Figure 6 shows a time series of northern hemisphere 850 hPa temperature scores for day 5 forecasts from early February to late May. The impact is clearly at its maximum in March and April, fading away in May. Almost every single forecast with the new snow albedo is better than the control with the old albedo scheme. Scatter plots of forecasts for day 1, 3, 5 and 7 for all northern hemisphere continental areas display improvement in almost every forecast (not shown).

4. IMPROVEMENT OF MEAN THERMAL STATE IN LONG INTEGRATIONS

An ensemble of 9 members of 120-day forecasts at resolution T63L31 were run with initial dates between 960130 and 960207. The mean difference between new and old albedo schemes is shown for March-April-May in Figure 7. The lower panel shows the 850 hPa temperature difference with contours of 1K. A large warming of more than 4K over northeastern Asia, and more than 2 degrees in Canada can be seen; the impact is significant at the 95% level. The upper panel shows the 500 hPa geopotential difference (contours in 10 dam), where there are corresponding local impacts over the continents, significant at the 95% level. Perhaps more surprising is to see the impact over the western Pacific at 500 hPa, where a more pronounced trough significantly reduces the model systematic error for this region (not shown).

Figure 8 differences the zonal mean temperature error of the new and control albedo forecasts for the last month (May) of the ensemble of 120-day integrations. The effect of the new snow albedo over the boreal forests is to produce a large warming from 45 to 80°N from the surface up to 600 hPa, largely eliminating the model cold bias in the lower troposphere at 60°N. This shows that the impact of the surface albedo change extends through a deep tropospheric layer. There is a moistening of up to 0.5 gkg^{-1} in the same areas (not shown); while the impact on the zonal mean zonal wind is small (not shown).

5. Discussion and Conclusions

A change in the model snow albedo and its impact has been presented. While the previous snow albedo was of the order of 0.7 to 0.8 for relatively small snow depths, the new formulation has a deep snow albedo of 0.2 in boreal forest areas and 0.7 in forest-free areas. Results presented show a very large positive impact on the forecast 2-m temperatures in Spring, and a reduction of the lower tropospheric cold bias in Spring. Forecast impacts in the northern hemisphere are large and positive from February to May, and negligible for all other areas and seasons.

The new snow formulation was included in cycle 15R6, which became operational in December, 1996. Our final Figure 9 compares (with the same colour contours) the average March-April 850 hPa 5-day forecast temperature errors in the operational model for 1996 and 1997. At high northern latitudes the cold bias in Spring 1996 at 850 hPa was considerable, as high as -6K over eastern Russia. There was also a positive bias over China. In Spring 1997, with the new snow albedo scheme, the cold bias over the boreal forests has been almost eliminated, although a residual cold bias can now be seen near 40°N over Asia. These operational forecasts are for two different years, but it is clear that the change to the snow albedo scheme for the boreal forests has greatly reduced the model systematic temperature error in Spring in the northern hemisphere.

Future changes in the snow formulation, including a better vegetation distribution, a better handling of melting and an age dependent snow albedo and density should further improve on these results. Improvements are also needed in the handling of the snow evaporation, which is now overestimated for the boreal forest regions after this albedo change.

Acknowledgements

Alan Betts was supported by NASA under Grant NAG5-7377 and the National Science Foundation under Grant ATM95-05018. ECMWF provided travel support.

References

Betts, A.K., and J. H. Ball, 1997: Albedo over the boreal forest. *J. Geophys. Res., 102*, 28,901-28,913.

Dorman, J.L., and P.J. Sellers, 1989: A global climatology of albedo, roughness length and stomatal resistance for atmospheric general circulation models as represented by the Simple Biosphere Model (SiB). *J. Appl. Meteorol., 28*, 833-855.

Harding, R.J. and J.W. Pomeroy, 1996: The energy balance of the winter boreal landscape. *J. Clim.,9,* 2778-2787.

Laine, V., and M. Heikinheimo, 1996: Estimation of surface albedo from NOAA AVHRR data in high latitudes. *Tellus, 48A*, 424-441.

Pomeroy, K. W. and K. Dion, 1996: Winter snow radiation extinction and reflection from a pine canopy: Influence of intercepted snow. Paper presented at the 53rd Annual Eastern Snow Conference, Williamsburg, VA., May 1996.

Robinson, D.A., and G. Kukla, 1984: Albedo of a dissipating snow cover. *J. Clim. Appl. Meteorol.*, **24**, 402-411.

Robinson, D.A., and G. Kukla, 1985: Maximum surface albedo of seasonally snow-covered lands in the Northern Hemisphere. *J. Clim. Appl. Meteorol.*, *24*, 402-411.

Sellers, P.J., Meeson, B.W., J.W. Closs, J. Collatz, F.E. Corprew, D.Dazlich, F.G. Hall, Y. Kerr, R. Koster, S. Los, K. Mitchell, J.M.P. McManus, D.M. Myers, K.-J. Sun, and P. Try, 1996: The ISLSCP initiative I-global data sets: Surface boundary conditions and atmospheric forcings for land-atmosphere models. *Bull. Am.. Meteorol. Soc.*, *77*, 1987-2005.

Sellers, P.J. and 20 co-authors, 1997: BOREAS in 1997: Experiment overview, scientific results and future directions, *J. Geophys. Res.*, *102*, 28 731-28 769.

Viterbo, P. and A.C.M. Beljaars, 1995: An improved land-surface parameterization in the ECMWF model and its validation. *J. Clim.*, *8*, 2716-2748.

Viterbo P., A.C.M. Beljaars, J.-F. Mahfouf and J. Teixeira, 1998: Soil moisture freezing and its interaction with the boundary layer. *Q. J. R. Meteorol. Soc.* (submitted).

APPENDIX: THE TWO MODEL ALBEDO SCHEMES

In the operational model prior to December 1996, the snow albedo was derived from a fairly complex series of computations, involving background albedo, snow depth, roughness length, vegetation fraction, surface temperature, and interception reservoir contents. However when the intermediate results of this computation were carefully checked in typical winter and spring situations, it was clear that the end result was unsatisfactory. First an estimate of the fraction of the vegetation covered by snow was made, based on the roughness length for momentum. However over the boreal forest the implicit masking of snow by vegetation is small. An effective snow covered fraction of the grid box is also calculated, based on the snow water equivalent depth, but in winter for the boreal forest, this value is very rarely different from 1. The albedo of the snow part of the grid box increases from a minimum of 0.4 at soil temperatures of 0°C, to a maximum of 0.8 below -5°C. Given the large cold bias in the model (before the 1996-97 winter), this value is most of the time around 0.8. A first estimate of the grid-box albedo is made by combining the background albedo with the snow albedo, based on the effective fraction defined above. Finally, this estimate can be further increased in the presence of ice dew, which brings the albedo up to 0.8 in some areas that were still below this value. The end result of all the above computations is an albedo in the presence of snow that is rarely outside the 0.7-0.8 range, as shown earlier in Figure 3b.

In the new scheme, an albedo for the snow covered part of the grid box, α_S (defined by equation (1) in section 2.2), ensures a deep snow albedo of 0.2 for forest covered areas (background albedo smaller than 0.13), of 0.7 for forest-free areas (background albedo larger than 0.15), and a linear relationship linking the two. The fraction of the grid box covered by snow is given by

$$C_s = \min(1, Sn / Sn_c) \qquad Sn_c = 0.015 \tag{2}$$

where Sn_c is the snow amount in metres of equivalent water. A first estimate of the grid box albedo, α_*, is given as a linear combination of the Eq. (1) and the background albedo,

$$\alpha_* = C_s \alpha_s + (1 - C_s)\alpha_B \tag{3}$$

In order to obtain the final forecast albedo, α_F, an ice dew correction is added for forest free areas

$$\alpha_F = \max(\alpha_D, \alpha_*) \tag{4}$$

$$\alpha_D = 0.4 f_1 f_2 C_l$$

$$f_1 = \min\left(1, \max\left(0, \frac{\alpha_B - b_1}{b_1 - b_2}\right)\right), f_2 = \min\left(1, \max\left(0, \frac{T_o - T_s}{5}\right)\right)$$

In Eq. (4), T_s, and T_o, represent respectively the soil temperature and the freezing temperature, while C_l is the fraction of the grid box covered by the interception reservoir, defined in *Viterbo and Beljaars* [1995].

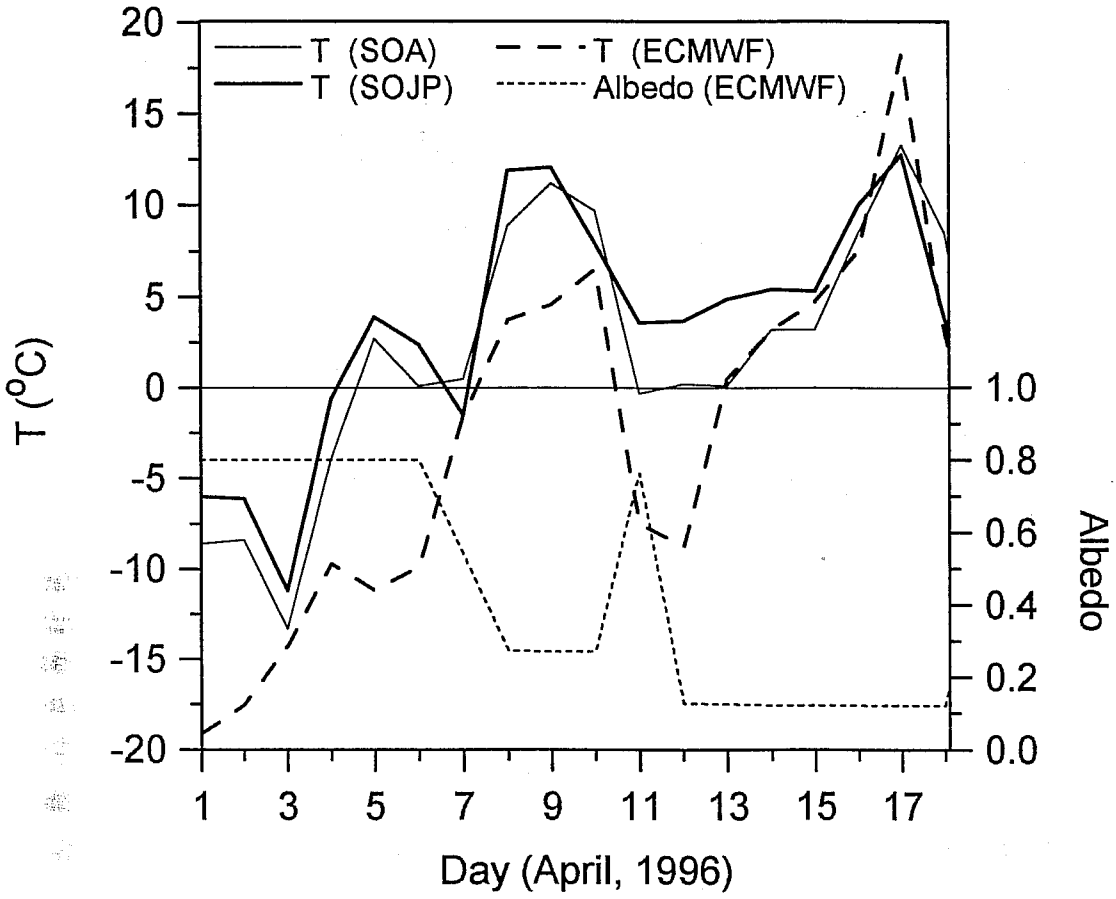

Fig. 1 Time series of observed and ECMWF model forecast 2-m temperatures at 0000 UTC for BOREAS southern study area Old Aspen and Old Jack Pine sites, together with model albedo.

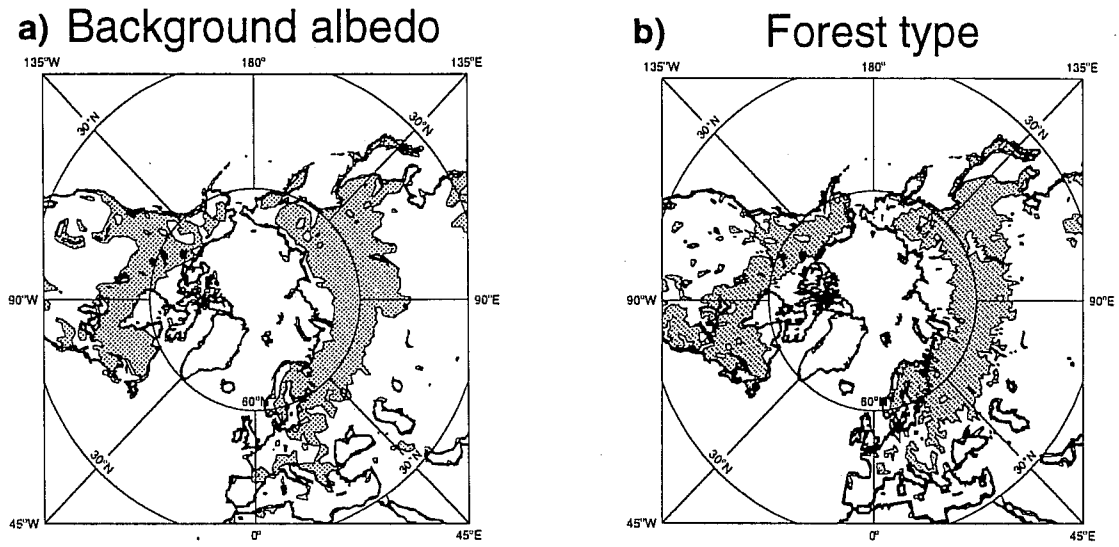

Fig. 2 a) Background albedo. Shaded values over land represent values smaller than 0.15
b) ISLSCP Initiative I vegetation type. Shaded values over land represent all types of forest.

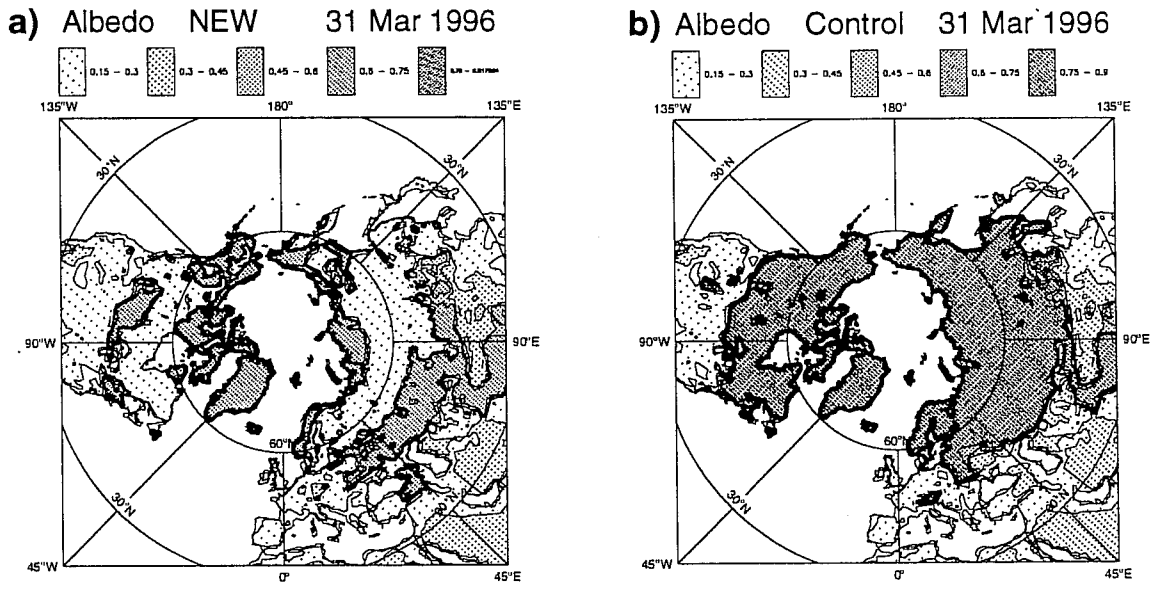

Fig. 3 a) Forecast albedo for 960331for new albedo and b) old albedo model.

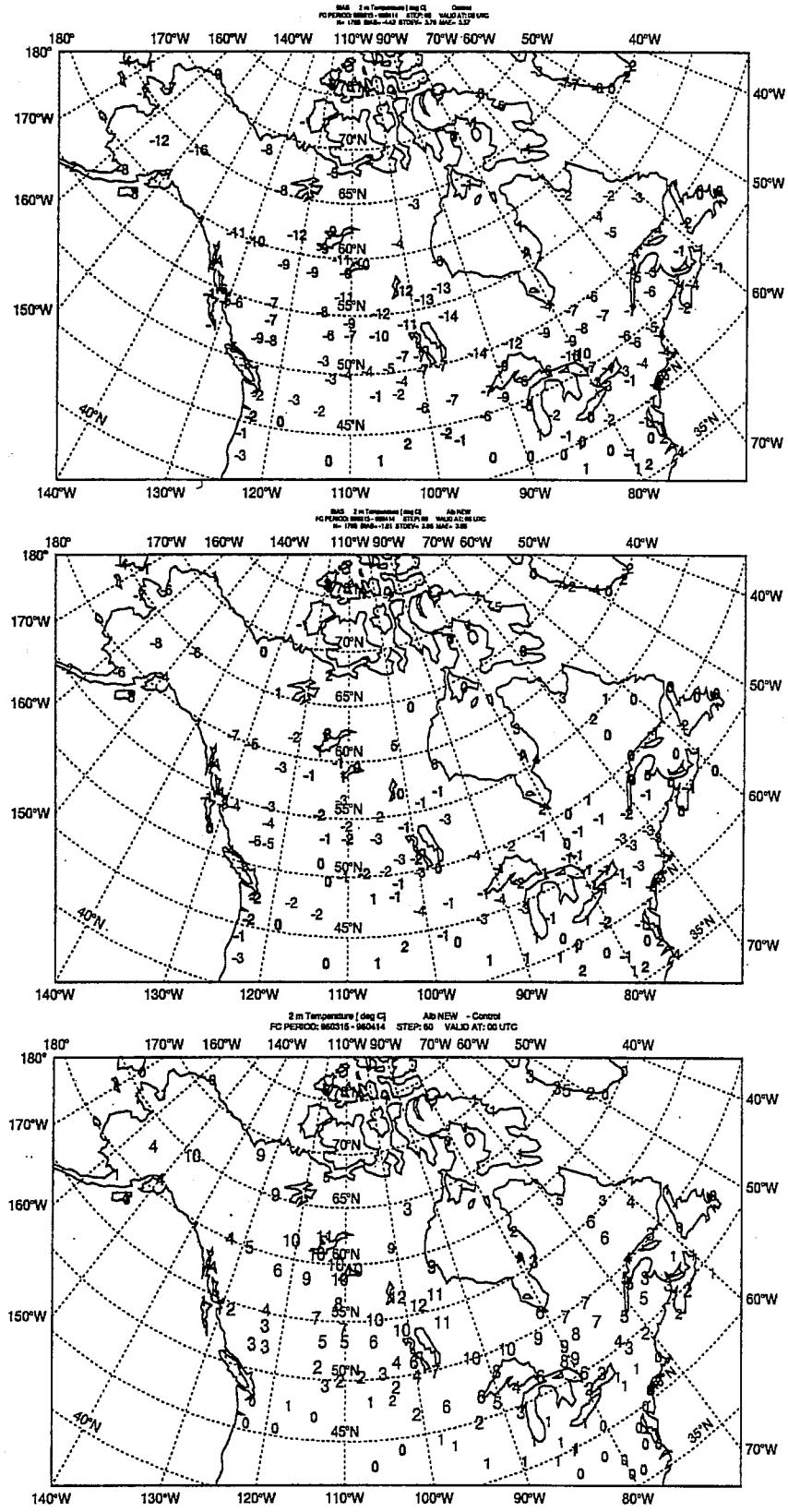

Fig. 4 Verification of 2m temperature over North America, for the 11 T106L31 forecasts with initial dates between 960315 and 960414.
a) Top: CONTROL 15R5; b) Middle: NEW snow albedo 15R6; c) Bottom: difference NEW–CONTROL.

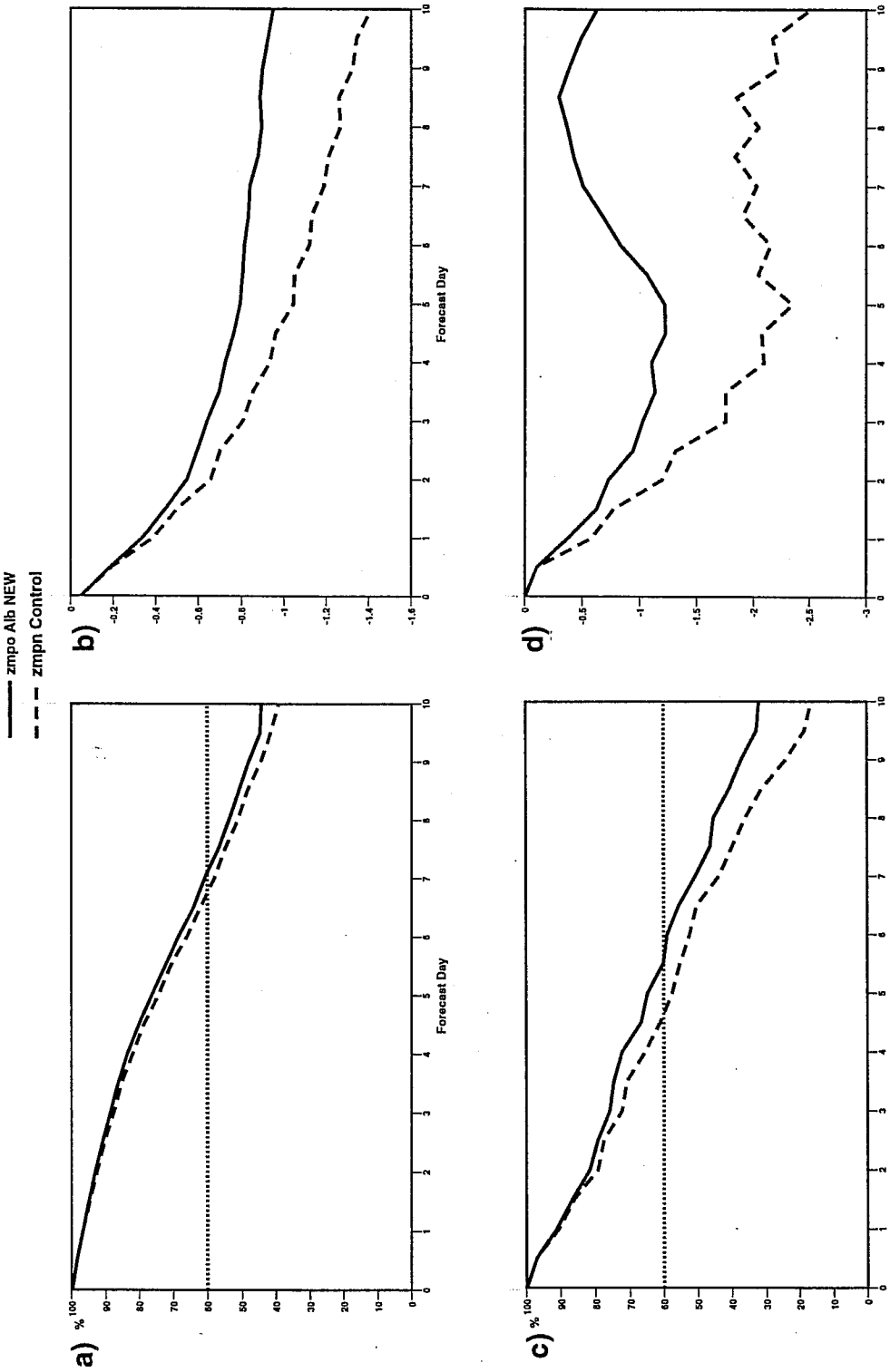

Fig. 5 Mean objective scores for 850 hPa temperature for the 20 T106 forecasts with initial dates between 960303 and 960429. For each area the anomaly correlation (left), and bias (right) are shown. a) Northern Hemisphere (top) and (b)Eastern Asia (bottom)

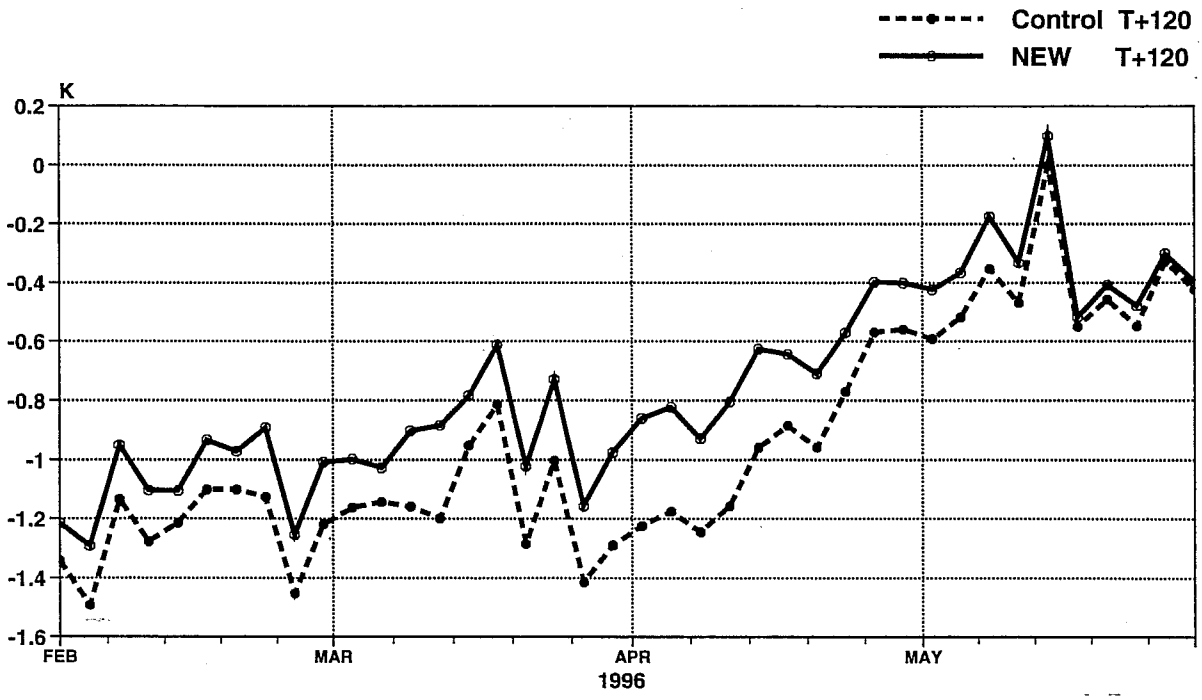

Fig. 6 Time series of bias of 850 hPa northern hemisphere temperatures for the forecasts with initial dates between 960202 and 960529.

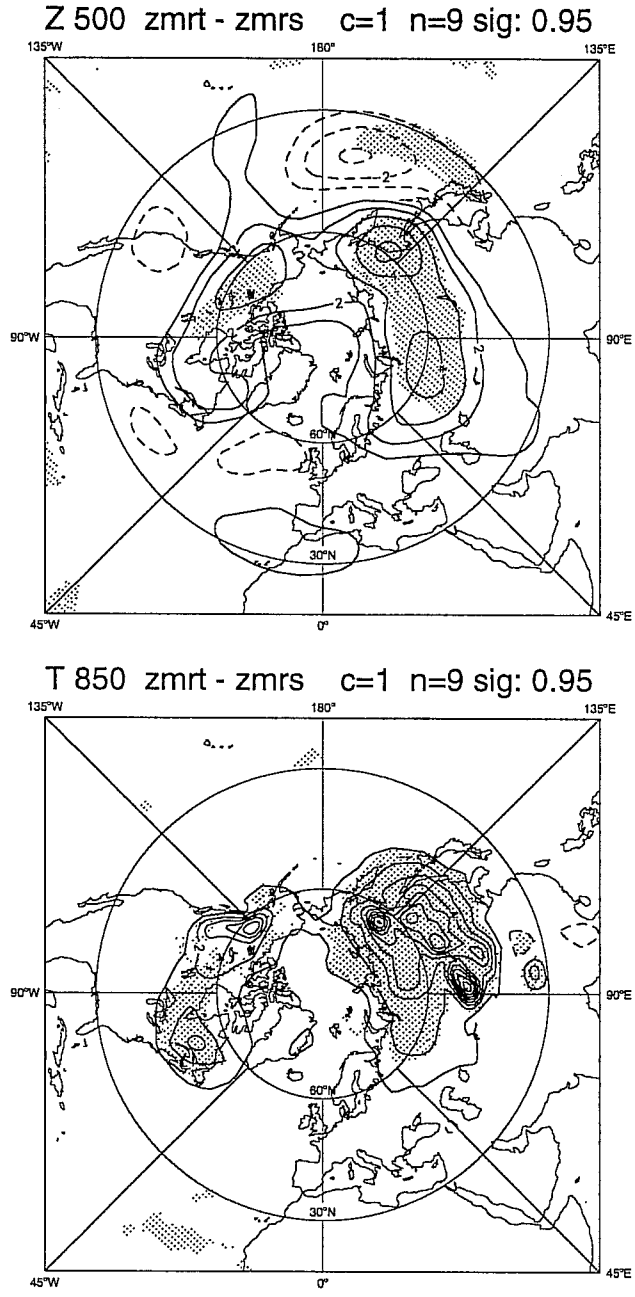

Fig. 7 March-April-May mean difference of 850 hPa temperature (top) and 500 hPa geopotential for NEW 15R6 - CONTROL 15R5 for an ensemble of nine T63L31 integrations, starting near the beginning of February. Shaded areas in the difference plot correspond to significant differences at 95% level.

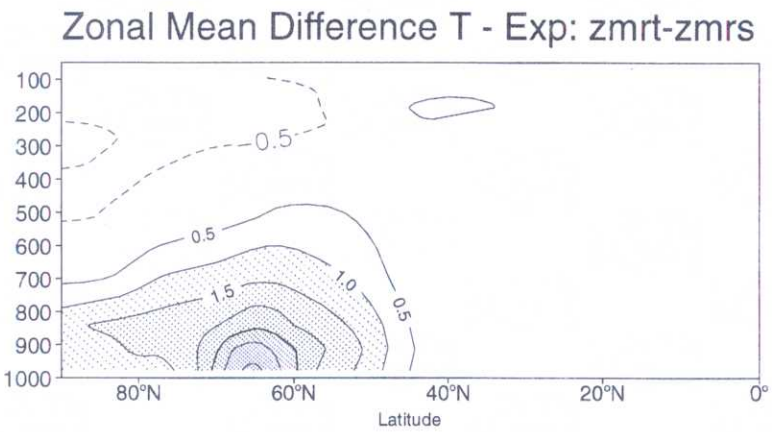

Fig. 8 Zonal mean temperature difference (NEW-CONTROL) for northern hemisphere for the last month (May) for the ensemble of nine T63L31 120-day integrations.

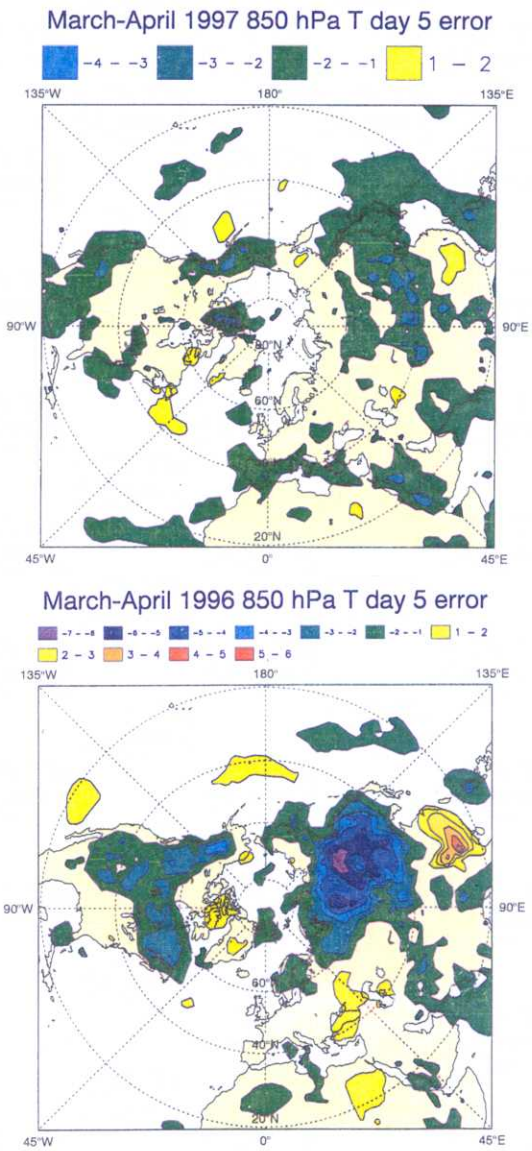

Fig. 9 Comparison of the average 5-day forecast temperature errors at 850 hPa in the ECMWF operational model for March-April 1996 and 1997.